Sensors and Materials, Vol. 18, No. 8 (2006) 395–404
MYU Tokyo

S & M 0658

Measurement of Oxygen Potential of Stainless Steel Slags with a Pt Electrode-Based Sensor Prepared by MOCVD

Víctor Arredondo-Torres, Antonio Romero-Serrano*, Roberto Vargas-García, Beatriz Zeifert, José Hallen-López and Mayra Figueroa-Torres[1]

Metallurgy and Materials Department, IPN-ESIQIE, A. P. 118-431, Mexico D.F. 07051
[1]Chemical and Materials Department, CIMA.

(Received May 25, 2006; accepted December 6, 2006)

Key words: metal-organic chemical vapor deposition, oxygen sensor, Pt film, stainless-steel slags

A sensor employing yttria-stabilized zirconia (YSZ) was used to determine the oxygen potential of slags based on the $CaO\text{-}SiO_2\text{-}CaF_2\text{-}CrO_X\text{-}Al_2O_3$ system at 1723 K. The YSZ sensors were coated with Pt electrode films deposited by metal-organic chemical vapor deposition (MOCVD) to increase the conductivity of the measuring devices and to decrease their response time. The oxygen potential of the slags was related to the $a_{CrO}/a_{CrO1.5}$ ratio through the Nernst equation and the free energy of the equilibrium reaction between CrO and Cr_2O_3. Good agreement was obtained between the measured values and the theoretically calculated results. The order of magnitude of $a_{CrO}/a_{CrO1.5}$ was too low, between 0.0005 and 0.005, owing mainly to the high oxidation conditions that prevail in an open induction furnace. It was also found that $a_{CrO}/a_{CrO1.5}$ slightly decreases with an increase in the amount of Al_2O_3 in the system.

1. Introduction

The slags used in stainless-steel production contain transition metallic ions of chromium, which respond to oxygen potential variations by changing the oxidation state. The solubility of chromium oxide directly influences the metallurgical process because a high solubility increases chromium losses in the slags. Since chromium is one of the major constituents of stainless steels, it represents a large portion of the raw-material cost. Consequently, high chromium recoveries are essential for the economy of the overall

*Corresponding author, e-mail address: romeroipn@hotmail.com

process and also for reducing the eventual polluting effects of chromium-containing slags and wastes.[1]

Chromium-oxide-containing systems are more complex than other transition-metal-oxide systems, such as iron-containing systems, because chromium exists in three valencies, Cr^{2+}, Cr^{3+} and Cr^{6+}, depending on the oxygen partial pressure, temperature and slag composition.[2] Divalent and trivalent chromium coexist in the slags related to ferrochromium and stainless-steel production.

The behavior of chromium and its oxides as well as the measurement of the oxygen potential in steelmaking slags have been the subject of several studies concerned with equilibrium behavior. Some of these studies carried out in situ measurements based on the electrochemical determination of the oxygen potential in the slag melt using yttria-stabilized zirconia (YSZ) as an oxygen-ion conductor.[3,4]

YSZ sensors have been successfully used to measure gases in air such as CO, SO_2 and NO_x at relatively low temperatures (600–650°C).[5] Platinum is widely used as the electrode material in these sensors because of its electrocatalytic nature, which promotes charge transfer reactions at the electrolyte/electrode interface. Usually, porous Pt electrodes are prepared by firing Pt paste at around 900–1200°C; however, highly catalytic Pt electrodes can also be prepared by an appropriate deposition technique (sputtering or CVD) on the surface of the solid electrolyte.[6] It has been shown that highly catalytic Pt electrodes improve the response time of YSZ sensors.[7]

In this study we have prepared YSZ sensors to estimate the oxygen potential and the CrO/Cr_2O_3 activity ratio in slags based on the $CaO\text{-}SiO_2\text{-}CaF_2\text{-}CrO_X\text{-}Al_2O_3$ system at 1723 K. To improve the efficiency and response time of these oxygen sensors, Pt electrode films were prepared by MOCVD.

2. Experimental Procedure

2.1 *Oxygen sensor*

YSZ sensors were prepared by blending 91 g of YSZ, ZrO_2-8%Y_2O_3 (TOSOH®, TZ-8Y) with 50 cm^3 of a solution of 0.01M $NaNO_3$ and 3.5 cm^3 of ammonium polyacrylate as a dispersant. The body of the sensor was prepared by slip casting in a plaster of paris mold, followed by sintering in air at 1873 K for 2 h. The sensor was shaped in the form of a 5-cm-long open-ended tube with an outside diameter of 8 mm.

The YSZ tubes were coated over their entire surfaces with Pt electrode films using a horizontal hot-wall MOCVD apparatus, which has been described elsewhere.[8] The Pt films were carefully removed from the open edge of the tubes, using 400-grade emery paper, to form a working electrode on the external surface and a reference electrode on the internal surface of the tubes. Platinum-acetylacetonate [$(CH_3\text{-}COCHCO\text{-}CH_3)_2Pt$] was used as a precursor and its vapors were carried by an argon gas flow to the reactor chamber. Porous Pt films were obtained under the following deposition conditions: precursor temperature, T_{prec} = 443 K; deposition temperature, T_{dep} = 673 K; total gas pressure, P_{tot} = 133 Pa.

The reference electrode used was a mixture of Cr and Cr_2O_3 encased in a stabilized zirconia electrolyte thimble. Then the reference oxygen partial pressure was fixed by the establishment of the chemical equilibrium

$$Cr + \tfrac{3}{4}O_2 = \tfrac{1}{2}Cr_2O_3. \quad (1)$$

The Gibbs energy of the reaction in eq. (1) can be expressed as

$$\Delta G^0_1 = -RTIn\left(\frac{\left(a_{Cr_2O_3}\right)^{1/2}}{\left(a_{Cr}\right)\left[pO_2\right]^{3/4}}\right). \quad (2)$$

The standard Gibbs energy of the reaction, calculated from the thermochemical data compiled by Barin,[9] is given as

$$\Delta G^0_1 = -556084.9+122.8T \text{ J}. \quad (3)$$

As the activities of the oxide and the metal are unity, the partial pressure of oxygen is fixed for a given temperature.

With this type of electrode, the value of the oxygen potential at the slag/electrolyte interface is ill-defined because it involves oxygen transfer across the electrolyte wall to or from the reference electrode Cr-Cr_2O_3. The Pt-film YSZ-based sensor for detecting oxygen in slag is shown schematically in Fig. 1.

The electrochemical properties of Pt electrode films on YSZ were investigated by impedance spectroscopy in the frequency range of 10^5–10^{-2} Hz using a Solartron 1255 frequency-response analyzer from 573 to 1073 K in air. The structure of the Pt layer was analyzed using a Bruker D8 Focus X-ray diffractometer. A Jeol 6300 scanning electron microscope with an accelerating voltage of 25 kV was used to measure the particle size of

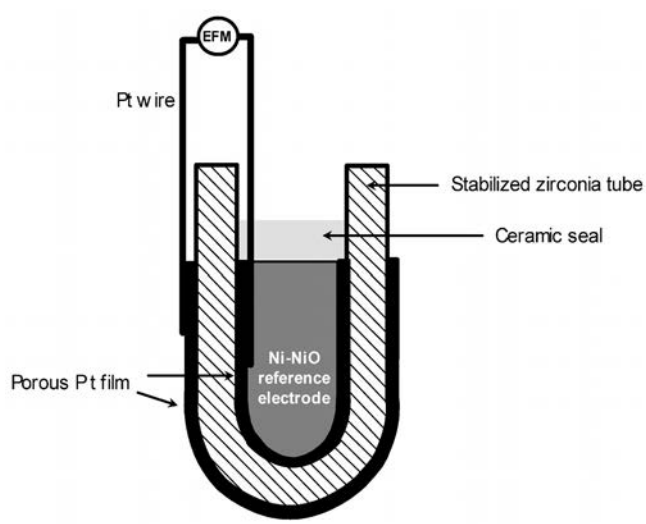

Fig. 1. Cross-sectional view of YSZ-based sensor with Pt electrode films prepared by MOCVD.

the Pt film and its thickness.

The measurement of oxygen potential is based on the use of a YSZ electrochemical cell, which can be represented as

$$Pt|O_2(slag)||ZrO_2(Y_2O_3)||Cr\text{-}Cr_2O_3|Pt\ . \tag{4}$$

When immersed in molten slag, the cell produces an EMF as a result of the difference in oxygen potential between the two sides of the solid electrolyte according to Nernst's law:

$$EMF = \frac{RT}{4F} \ln\left(\frac{pO_{2(slag)}}{pO_{2(ref)}}\right), \tag{5}$$

where $pO_{2(ref)}$ is the oxygen partial pressure of the reference electrode, $pO_{2(slag)}$ is the oxygen partial pressure in the slag, T is the absolute temperature, R is the gas constant and F is the Faraday constant. The oxidation-reduction reaction in slag may be represented by

$$4CrO+O_2 = 4CrO_{1.5}. \tag{6}$$

The Gibbs energy of the reaction in eq. (6) can be expressed as

$$\Delta G^0{}_6 = -RT\ln\left(\frac{\left(a_{CrO_{1.5}}\right)^4}{\left(a_{CrO}\right)^4\left[pO_{2(slag)}\right]}\right). \tag{7}$$

Equation (7) can be changed to

$$\left(\frac{a_{CrO}}{a_{CrO_{1.5}}}\right) = \left[\frac{1}{pO_{2(slag)}}\exp\left(\frac{\Delta G^0{}_6}{RT}\right)\right]^{1/4}. \tag{8}$$

The standard Gibbs energy of the reaction in eq. (6), calculated from the thermochemical data compiled by Barin,[9] is given as

$$\Delta G^0_6 = -891487+273.52T\ J. \tag{9}$$

Here, pure liquid was chosen as the standard state for both CrO and $CrO_{1.5}$. Then, this value was used in deriving the thermodynamic relation between the oxygen potential in the slag and the sensor EMF reading.

2.2 *Material, apparatus and procedure*

The experiments were carried out at 1723±10 K using 50 g of slag and a platinum crucible of 25 mm inner diameter and 35 mm height. The slag was prepared with laboratory-reagent-grade compounds (CaO, Al_2O_3, CaF_2, SiO_2 and Cr_2O_3), which were previously ground into fine powder whose mean particle size was between 45 and 74 μm. The Al_2O_3 content ranged from 3 to 9 mass%, Cr_2O_3 and CaF_2 were 10 mass% each, and the slag basicity (B), defined as the ratio of CaO content to SiO_2 content (all mass%), was maintained at 1.5. The required powders were homogeneously mixed and placed into a Pt crucible. The working crucible was placed in a corundum protecting crucible and the slag was melted in an open induction furnace.

The melting temperature was measured with an R-type thermocouple (Pt-Pt, 13%Rh). After the required temperature was attained, the oxygen sensor was introduced into the liquid slag. The temperature and EMF of the oxygen sensor were recorded during the experiments.

The working and reference electrodes of the oxygen sensor have Pt films with superior electrochemical performance to promote equilibrium in the cell. This enabled the determination of the level of oxygen potential based on the Nernstian response of the sensor and the $a_{CrO}/a_{CrO1.5}$ ratio through eq. (8). To check the reproducibility, some of the trials were carried out twice.

2.3 *Thermodynamic analysis*

Thompson et al.[10] have developed a thermodynamic database available in the software FACTSage (Facility for the Analysis of Chemical Thermodynamics), which accesses databases of species in solution and allows the determination of the equilibrium composition and thermodynamic properties of a multiphase and multicomponent system at given temperature, pressure and initial composition. This software uses the quasi-chemical approximation[11] for liquid silicate slags. Thompson et al. reported that for the cases when Cr is present, all available data have been fully optimized for the $CaO\text{-}SiO_2\text{-}CrO_X\text{-}Al_2O_3$ system. Then, equilibrium computations were performed to estimate the effect of Al_2O_3 content on $a_{CrO}/a_{CrO1.5}$ in the $CaO\text{-}SiO_2\text{-}CaF_2\text{-}CrO_X\text{-}Al_2O_3$ system with slag compositions, oxygen partial pressure and temperatures similar to those of the experimental trials of this study.

3. Results and Analysis

3.1 *Pt-film characterization*

Figure 2 shows the A.C. impedance spectrum in air at temperatures as low as 723 K for Pt electrode films prepared by MOCVD on a YSZ substrate. The spectrum is presented at a temperature well below the normal operating temperatures of the materials, in order to bring the spectral features into the instrumental frequency range. The results were analyzed using the three components: bulk, grain boundary and interfacial reaction and/or diffusion-limited process. The small semicircle at a high frequency was attributed to the bulk response due to the small associated capacitance (10^{-12} F), which resembles that of a classical zirconia solid electrolyte.[12,13] The large semicircle in the low-frequency region

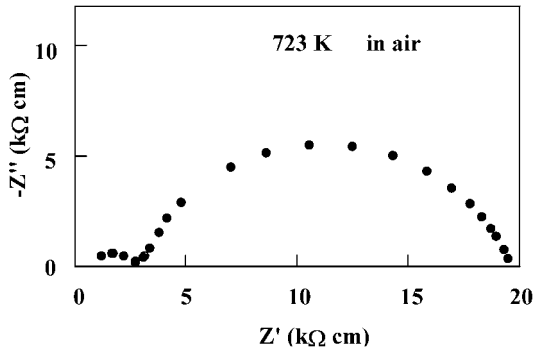

Fig. 2. Impedance spectrum at 723 K of Pt electrode films deposited on YSZ substrate.

was associated with charge transfer reactions at the electrode-electrolyte interface because of the capacitance values of 10^{-7}–10^{-6} F.[12,13] The grain boundary effect was too small to be resolved at 723 K.

Figure 3 shows the Arrhenius plot for the conductivity in relation to the total electrode resistance for Pt electrode films prepared by MOCVD on the YSZ substrate. The conductivity depends on the physical dimensions of the electrode; in this work we prepared Pt films that were about 7 μm thick and a porous electrode structure on the YSZ surface, which determines the regions of the three phases (oxygen-electrode-electrolyte) of contact. The total electrode resistance is represented by the charge transfer component. Pt films exhibit a higher conductivity than conventional Pt paste electrodes at temperatures below 1173 K.[14]

Previous Auger results have shown that Pt films prepared by MOCVD contain carbon impurities.[8] It is expected that the carbon content in the film will be eliminated during the preheating step of the sensor. Thus, at the test temperature (1723 K) the Pt electrode film will contain only a porous Pt film with high conductivity and high catalytic activity.

X-ray diffraction (XRD) patterns corresponding to the Pt-film YSZ substrate and the YSZ substrate without a Pt film are shown in Figs. 4(a) and 4(b), respectively. As can be observed, metallic-platinum Bragg reflections appear on the diffractogram. An X-ray diffraction pattern of the cubic structure of the YSZ substrate, Fig. 4(b), is included for comparison with the reflections of Pt and YSZ. It must be stressed that the broader Pt diffraction peak at 40.1° reveals the presence of platinum nanoparticles.

The sample was mounted and the microstructure was examined in detail by optical microscopy as well as SEM analysis. The SEM micrograph in Fig. 5(a) shows that the Pt film prepared by CVD produced a particle size in the range of 80–140 nm. Figure 5(b) shows a cross section of the Pt film on the YSZ substrate. The depth of the Pt film measured by SEM analysis was about 7 μm.

The sensor had a response time of about 3 s and the EMF stabilized in less than 2 min. The fact that the response time was so short in the experiments was attributed to the Pt electrode films deposited on YSZ, which increased the electrode conductivity of the sensors compared with that of conventional YSZ sensors.

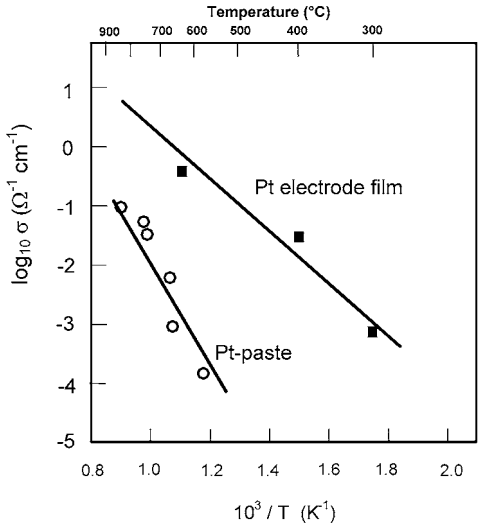

Fig. 3. Arrhenius plots for the conductivity in relation to the total electrode resistance for MOCVD Pt and Pt-paste-based electrodes.[14]

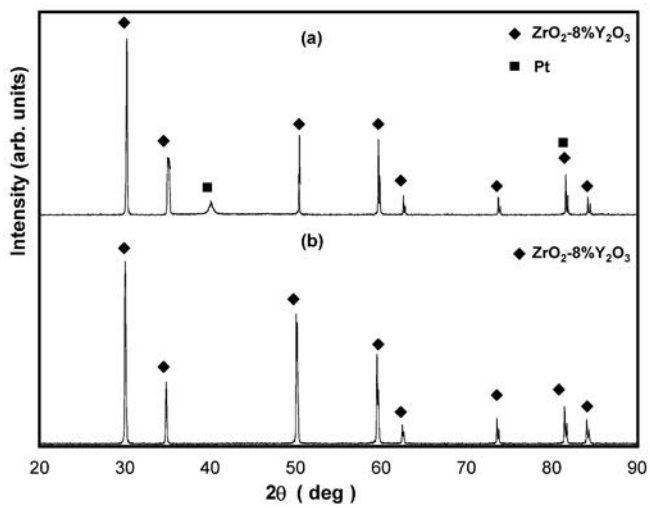

Fig. 4. XRD patterns corresponding to (a) Pt-film YSZ substrate and (b) YSZ substrate without Pt film.

3.2 *Experimental results*

The behavior of chromium and its oxides in steelmaking slags has been the subject of numerous studies;[2,15,16] however, the behavior of different chromium oxides in slags is poorly known. Most of these studies have been carried out at very low oxygen partial pressures, between 10^{-9} and 10^{-13} atm. That is why we have decided to compare $a_{CrO}/a_{CrO1.5}$ obtained using the electromotive force with those calculated theoretically using the thermodynamic package FACTSage. Table 1 shows the experimental EMF results as well as $a_{CrO}/a_{CrO1.5}$ calculated with eq. (8).

Figure 6 shows the experimental and calculated results of the effect of Al_2O_3 content in

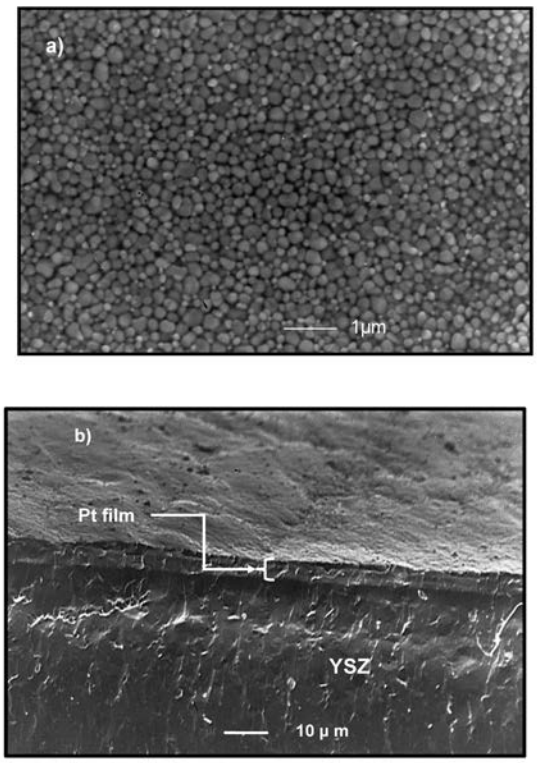

Fig. 5. Micrographs produced by SEM of Pt film processed by MOCVD. (a) Pt nanoparticles attached on the YSZ substrate and (b) cross section of Pt film.

Table 1
Experimental EMF and $a_{CrO}/a_{CrO1.5}$ for slags with 3, 6 and 9% Al_2O_3.

	3% Al_2O_3			6% Al_2O_3			9% Al_2O_3		
Time (min)	T (K)	EMF (V)	$a_{CrO}/a_{CrO1.5}$	T (K)	EMF (V)	$a_{CrO}/a_{CrO1.5}$	T (K)	EMF (V)	$a_{CrO}/a_{CrO1.5}$
0	1725	0.895	0.00480	1721	1.097	0.00121	1721	1.128	0.00098
1	1728	0.902	0.00465	1730	1.102	0.00123	1719	1.120	0.00102
2	1730	0.901	0.00476	1733	1.107	0.00121	1723	1.117	0.00107
3	1732	0.911	0.00448	1713	1.077	0.00132	1731	1.109	0.00118
4	1731	0.906	0.00461	1728	1.087	0.00135	1732	1.100	0.00126
5	1730	0.906	0.00459	1728	1.083	0.00138	1717	1.104	0.00113
6	1727	0.897	0.00480	1713	1.066	0.00142	1717	1.090	0.00124
7	1725	0.899	0.00467	1726	1.083	0.00137	1732	1.094	0.00131
8	1729	0.898	0.00482	1732	1.081	0.00143	1731	1.103	0.00123
9	1731	0.902	0.00474	1721	1.073	0.00142	1733	1.112	0.00117
10	1729	0.898	0.00480	1733	1.079	0.00146	1730	1.102	0.00123

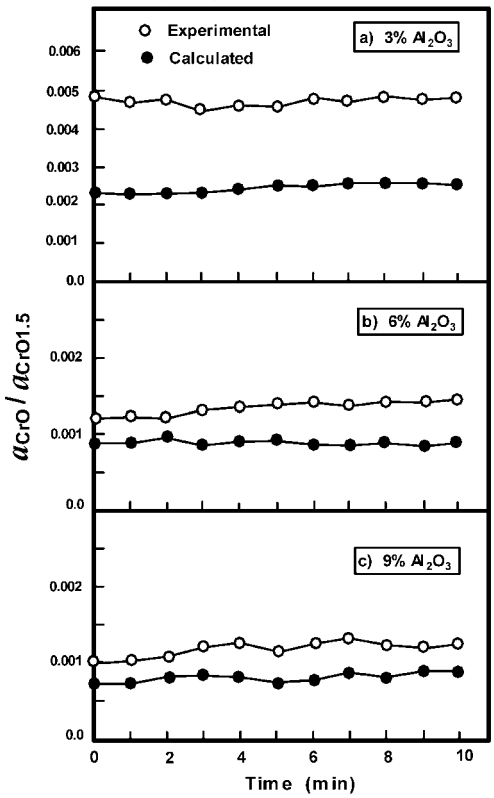

Fig. 6. Comparison of $a_{CrO}/a_{CrO1.5}$ measured using Pt-film YSZ-based sensor and results obtained through thermodynamic calculations.

the slag on $a_{CrO}/a_{CrO1.5}$ at 1723 K. The trend of both measured and calculated slag values is similar. The scatter in the points is due to variations in the experimental temperature, which was 10 degrees greater or less than 1723 K. Good agreement was obtained between the calculated and experimental results, although a strict comparison gives some discrepancies, which were attributed to the fact that the thermodynamic data for the liquid slag was extrapolated to the temperature and composition considered in this study. Besides, the FACTSage dabatases do not include CaF_2 as a component in the slag.

The order of magnitude of both the theoretically calculated and experimental $a_{CrO}/a_{CrO1.5}$ is too low, between 0.0005 and 0.005, owing mainly to the high oxidation conditions that prevail in the open induction furnace. It is clear that the oxygen partial pressure of the system has marked effects on both the activities of chromium oxides and the trivalent chromium fraction in the slags. The higher the oxygen partial pressure, the higher the trivalent chromium fraction and the lower the $a_{CrO}/a_{CrO1.5}$ ratio.

Xiao and Holappa[17] have reported that the Al_2O_3 content in the slag decreases the divalent chromium fraction; this is in agreement with the results shown in Fig. 6, where $a_{CrO}/a_{CrO1.5}$ decreases as a function of the amount of Al_2O_3 in the system.

4. Conclusions

A sensor employing yttria-stabilized zirconia coated on its surfaces with Pt electrode films deposited by MOCVD was used to measure the oxygen potential and $a_{CrO}/a_{CrO1.5}$ ratio of slags based on the CaO-SiO_2-CaF_2-CrO_X-Al_2O_3 system at 1723 K. Characterization of the oxygen sensor shows that the Pt film prepared by MOCVD produced a particle size in the range of 80–140 nm and a layer of about 7 μm depth. It was found that these Pt films exhibit a higher conductivity and catalytic activity than conventional Pt paste electrodes.

The $a_{CrO}/a_{CrO1.5}$ results calculated using the EMF are in good agreement with those obtained from the thermodynamic software FACTSage. The order of magnitude of $a_{CrO}/a_{CrO1.5}$ is too low, between 0.0005 and 0.005. It was found that $a_{CrO}/a_{CrO1.5}$ decreases when the amount of Al_2O_3 is increased or when the oxygen partial pressure is increased.

Acknowledgements

The authors wish to thank the institutions CONACyT, SNI, COFAA and Instituto Politecnico Nacional for the permanent assistance of the Process Metallurgy Group at the ESIQIE Metallurgy and Materials Department.

References

1 B. B. Lind, A. M. Fallman and L. B. Larsson: Waste Management **21** (2001) 255.
2 Y. Xiao, M. Reuter and L. Holappa: Proc. 6th Int. Conf. on Molten Slags, Fluxes and Salts. Stockholm, Sweden and Helsinki, Finland, (2000) 1.
3 E. T. Turkdogan: Ironmaking and Steelmaking **27** (2000) 32.
4 S. Smets, J. Janssens, B. Coletti, J. Plessers, B. Blanpain and P. Wollants: Proc. 6th Int. Conf. on Molten Slags, Fluxes and Salts (South Africa, 2004) p. 687.
5 N. Miura, G. Lu and N. Yamazoe: J. Electrochem. Soc. **143** (1996) L33.
6 I. Natali-Sora, C. Schmid and C. M. Mori: Proc. 17th Riso Int. Symp. on Materials Science: High Temperature Electrochemistry: Ceramics and Metals (Riso National Laboratory, Roskilde, Denmark, 1996) p. 369.
7 A. Sharma and P. D. Pacey: J. Electrochem. Soc. **140** (1993) 2302.
8 T. Goto, R. Vargas and T. Hirai: J. de Phys. IV **C3-3** (1993) 701 (in French).
9 I. Barin: Thermochemical Data of Pure Substances 436, ed. VCH Verlagsgesellschaft (Weinheim, 1989) p. 1093.
10 W. T. Thompson, C. W. Bale and A. D. Pelton: FACTSage-Facility for the Analysis of Chemical Thermodynamics, User's Manual (2005).
11 A. D. Pelton and M. Blander: Metall. Trans. B **17B** (1986) 805.
12 J. T. Irvine, D. C. Sinclair and A. R. West: Adv. Mater. **2** (1990) 132.
13 E. Barsoukov and J. R. Macdonald: Impedance Spectroscopy Theory, Experiment and Applications (Wiley-Interscience, New York, 2005) p. 238.
14 S. P. S. Badwal and H. J. De Bruin: Phys. Stat. Sol. **54** (1979) 261.
15 E. B. Pretorious, R. Snellgrove and A. Muan: J. Am. Ceram. Soc. **75** (1992) 1378.
16 Y. Xiao, L. Holappa and M. A. Reuter: Metall. Trans. B **33B** (2002) 595.
17 Y. Xiao and L. Holappa: ISIJ Int. **33** (1993) 66.